A&A 505, L13–L16 (2009)
DOI: 10.1051/0004-6361/200912713

Astronomy & Astrophysics

Letter to the Editor

Lithium in the globular cluster NGC 6397⋆,⋆⋆,⋆⋆⋆

Evidence for dependence on evolutionary status

J. I. González Hernández[1,2], P. Bonifacio[1,2,3], E. Caffau[1], M. Steffen[4], H.-G. Ludwig[1,2], N. T. Behara[1,2], L. Sbordone[1,2], R. Cayrel[1], and S. Zaggia[5]

[1] Cosmological Impact of the First STars (CIFIST) Marie Curie Excellence Team, France
[2] GEPI, Observatoire de Paris, CNRS, Université Paris Diderot, Place Jules Janssen, 92190 Meudon, France
e-mail: Jonay.Gonzalez-Hernandez@obspm.fr
[3] Istituto Nazionale di Astrofisica - Osservatorio Astronomico di Trieste, via Tiepolo 11, 34143 Trieste, Italy
[4] Astrophysikalisches Institut Potsdam, An der Sternwarte 16, 14482 Potsdam, Germany
[5] INAF – Osservatorio Astronomico di Padova, Vicolo dell'Osservatorio 5, Padua 35122, Italy

Received 17 June 2009 / Accepted 3 September 2009

ABSTRACT

Context. Most globular clusters are believed to host a single stellar population. They can thus be considered a good place to study the Spite plateau and to search for possible evolutionary modifications of the Li content.
Aims. We want to determine the Li content of subgiant (SG) and main sequence (MS) stars of the old, metal-poor globular cluster NGC 6397. This work was aimed not only at studying possible Li abundance variations but also to investigate the cosmological Li discrepancy.
Methods. Here, we present FLAMES/GIRAFFE observations of a sample of 84 SG and 79 MS stars in NGC 6397 selected in a narrow range of $B - V$ colour and, therefore, effective temperatures. We determine both effective temperatures and Li abundances using three-dimensional hydrodynamical model atmospheres for all the MS and SG stars of the sample.
Results. We find a significant difference in the Li abundance between SG stars and MS stars, the SG stars having an abundance higher by almost 0.1 dex on average. We also find a decrease in the lithium abundance with decreasing effective temperature, both in MS and SG stars, albeit with a significantly different slope for the two classes of stars. This suggests that the lithium abundance in these stars is, indeed, altered by some process, which is temperature-dependent.
Conclusions. The lithium abundance pattern observed in NGC 6397 is different from what is found among field stars, casting some doubt on the use of globular cluster stars as representative of Population II with respect to the lithium abundance. None of the available theories of Li depletion appears to satisfactorily describe our observations.

Key words. stars: abundances – stars: atmospheres – stars: population II – stars: fundamental parameters – Galaxy: globular clusters: individual: NGC 6397

1. Introduction

The old, metal-poor dwarf stars of the Galactic halo share approximately the same Li abundance, irrespective of their metallicity or effective temperature (Spite & Spite 1982a,b). This plateau of lithium was believed to provide evidence of a primordial Li abundance. The WMAP satellite has been able to measure with high accuracy the baryonic density from the fluctuations of the cosmic microwave background (Spergel et al. 2007). This result implies a primordial Li abundance of log(Li/H) + 12 = 2.72 ± 0.06 (Cyburt et al. 2008) whereas the observed Li abundances in metal-poor dwarfs are in the range 2.0–2.4 (see Sbordone et al. 2008; Bonifacio et al. 2007a; Asplund et al. 2006; Charbonnel & Primas 2005; Meléndez & Ramírez 2004, and references therein). This discrepancy may be trivially solved if the *Spite plateau* does not represent the primordial Li abundance. In this case the amount of lithium in the atmospheres of all ancient stars, of all masses and metallicities, must have been uniformly depleted by at least a factor of three.

Possible explanations of this difference are: (a) the first generation of stars, Population III stars, could have processed some fraction of the halo gas, lowering the lithium abundance (Piau et al. 2006); (b) the primordial Li abundance has been uniformly depleted in the atmospheres of metal-poor dwarfs by some physical mechanism (e.g. turbulent diffusion as in Richard et al. 2005; Korn et al. 2006; gravitational waves as in Charbonnel & Talon 2005, etc.); (c) the standard Big Bang nucleosynthesis (SBBN) calculations should be revised, possibly with the introduction of new physics (see e.g. Jedamzik 2004, 2006; Jittoh et al. 2008; Hisano et al. 2009). The observed Li abundances, A(Li), in

⋆ Based on observations obtained with FLAMES/GIRAFFE at VLT Kueyen 8.2 m telescope in programme 079.D-0399(A).
⋆⋆ Table and Figs. 3–10 are only available in electronic form at http://www.aanda.org
⋆⋆⋆ Table 2 is available in electronic form at http://www.aanda.org and at the CDS via anonymous ftp to cdsarc.u-strasbg.fr (130.79.128.5) or via http://cdsweb.u-strasbg.fr/cgi-bin/qcat?J/A+A/505/L13

metal-poor stars appear to show a very well defined plateau with very little dispersion at relatively high metallicities, whereas at low metallicities there seems to be an increased scatter, or perhaps even a sharp down turn in the Li abundances (Bonifacio et al. 2007a; González Hernández et al. 2008; Sbordone et al. 2008). The existence of a slope in A(Li) versus [Fe/H] would exacerbate the discrepancy between Li abundance in metal-poor stars and the WMAP predictions (Bonifacio et al. 2007a). The issue of the slope in the plateau is somewhat elusive and different groups reach different conclusions, depending on the adopted temperature scale (Meléndez & Ramírez 2004).

Globular clusters (GCs) were initially considered to be a good place to investigate the Spite plateau (Molaro & Pasquini 1994; Pasquini & Molaro 1996, 1997; Boesgaard et al. 1998), since the classical paradigm was that GCs are made of a single stellar population. The discovery of correlations among elemental abundances in turn-off (TO) stars (Gratton et al. 2001) and in particular the presence of a Li-Na anti-correlation (Pasquini et al. 2005; Bonifacio et al. 2007b), showed the need for the presence of different stellar populations, capable of nucleosynthetic activity and variable amounts of pollution of the presently observable stars. Such signatures are not found among field stars and are peculiar to GCs. This makes the perspective of using GCs to investigate the Spite plateau meagre.

Among the observed GCs, NGC 6397 occupies a special role, in the sense that the Li abundance among non-evolved stars is very homogeneous (Thévenin et al. 2001; Bonifacio et al. 2002), at variance with what is observed in NGC 6752 (Pasquini et al. 2005) and 47 Tuc (Bonifacio et al. 2007b). More recent studies (Korn et al. 2006, 2007) have claimed a tiny variation of A(Li) along the subgiant branch, in the sense of higher A(Li) being found for lower $T_{\rm eff}$ values. This variation is however quite small compared to what is observed in NGC 6752 and 47 Tuc.

In this Letter we present the result of the analysis of the first observations of Li in main sequence (MS) stars of a globular cluster.

2. Observations

We integrated NGC 6397 over 15 h with the multi-object spectrograph FLAMES-GIRAFFE (Pasquini et al. 2002) at the European Southern Observatory (ESO), using the 8.2-m Very Large Telescope, on 2007 April-July, covering the spectral range $\lambda\lambda$6400–6800 Å at a resolving power $\lambda/\delta\lambda \sim 17\,000$. The targets were selected using our own calibrated Johnson-Cousins B, V photometry, based on public images (ESO program 163.O-0741(C)) obtained with WFI at the ESO/MPI 2.2 m telescope on 14 May 1999. We chose SG and MS stars in the colour range $B - V = 0.6 \pm 0.03$, thus ensuring a narrow $T_{\rm eff}$ range (see Fig. 3 online). By swapping the fibres on the SGs we managed to observe over 9 h for about 80 MS stars and 2.5 h for roughly the same number of SGs. The resulting S/N ratio ~80–130 is the same for both sets of stars. The spectra were reduced using the ESO Giraffe pipeline, version 2.5.3. A combined spectrum of all sky fiber spectra in each night was properly subtracted from each individual spectrum. We then corrected each spectrum for the earth velocity and combined all the spectra of the same target (see the quality of the spectra in Fig. 4 online). Each star spectrum was corrected for its radial velocity, providing a mean cluster radial velocity of $V_{\rm r,c} = 18.5$ km s^{-1}. We removed all stars, considered as cluster non-members, with $|V_{\rm r} - V_{\rm r,c}| > 3\sigma_{V_{\rm r,c}}$, where $\sigma_{V_{\rm r,c}}$ is the radial velocity dispersion (3.7 km s^{-1}). We ended up with 79 MS (orginally 80) and 84 SG (88).

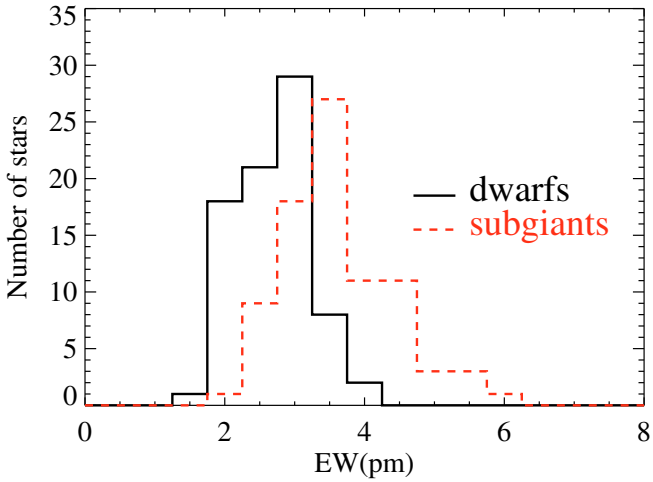

Fig. 1. Histograms of observed equivalent width of the lithium doublet at 670.8 nm in MS and SG stars in the globular cluster NGC 6397. Histograms of the equivalent width of Li line are displayed in bins of 0.5 pm for MS stars (solid line) and SG stars (dashed-dotted line).

3. Analysis and results

The narrow range in effective temperatures ensures that the uncertainty in the comparisons between MS and SG stars is dominated by the error on the measured equivalent width (EW) of the Li doublet line. These were measured by fitting the observed Li line profile with synthetic profiles of the Li doublet, as previously done for this cluster (Bonifacio et al. 2002). The EW measurements show (Fig. 1) that SGs have, on average, larger EWs of the Li doublet than MS stars (see the accuracy of our fitting procedure in Fig. 10 online). Although there is a slight dependence of the $B - V$ colour on surface gravity, and a SG star of a given colour is indeed cooler than a MS star of the same colour (~90 K at $B - V = 0.6$), the difference displayed in Fig. 1 is too large to be explained in this way. The weighted mean of the EW is 2.97 ± 0.02 pm and 4.06 ± 0.01 pm for MSs and SGs, respectively. The difference in the mean EW values is of about 1.1 pm which would require a mean $T_{\rm eff}$ difference of ~210 K. Prior to any model-dependent analysis, this clearly points towards the SGs having a higher Li abundance than the MSs. This is similar to what is found among field stars, where the Li abundance appears to be about 0.04 dex higher in turn-off and SG stars than in MSs (Charbonnel & Primas 2005).

We derived $T_{\rm eff}$ by fitting the observed Hα line profile with synthetic profiles, using 3D hydrodynamical model atmospheres computed with the CO^{5}BOLD code (Freytag et al. 2002; Wedemeyer et al. 2004). The ability of 3D models to reproduce Balmer line profiles has been shown in Behara et al. (2009), where the Hα profiles of the Sun, and the metal-poor stars HD 84937, HD 74000 and HD 140283 were investigated. From a purely theoretical point of view Ludwig et al. (2009) quantified the differences in using 1D or 3D models for Balmer line fitting (see the accuracy of our fitting procedure in Fig. 9 online). In the online Table 1 we provide information on the 3D model atmospheres used in this work. Self-broadening of the Hα line was calculated according to Barklem's theory (Barklem et al. 2000). Stark broadening was calculated following Griem's theories (Griem 1960) with corrections to approximate the Vidal et al. profiles (Vidal et al. 1973). Fixed values for the surface gravity were adopted for both SG and MS stars in the sample, according to the values that best match the position of the stars on a 12 Gyr isochrone (Straniero et al. 1997). The adopted

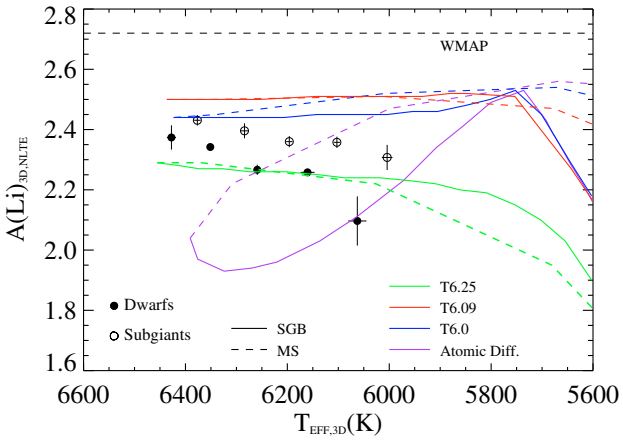

Fig. 2. 3D NLTE Li abundances versus 3D effective temperatures of the observed MS (filled circles) and SG (open circles) stars together with Li isochrones for different turbulent diffusion models. The stars have been divided into five effective temperature bins. The error bar in A(Li) shows the dispersion divided by the square root of the number of stars in each bin. In each isochrone, the dashed and solid stretch of the line shows the Li abundance in MS and SG stars, respectively. The horizontal dashed line depicts the cosmological Li abundance.

values were $\log(g/\mathrm{cm\ s^2}) = 4.40$ and 3.85 for MSs and SGs, respectively. This choice of the surface gravity is supported by the 1.6 mag difference in the V-filter between SGs and MSs in the sample. The Li abundances were derived using the same 3D hydrodynamical model atmospheres. The line formation of Li was treated in non-local thermodynamical equilibrium (NLTE) using the same code and model atom used in Cayrel et al. (2007). The model atom consists of 8 energy levels and 11 transitions. Full details will be given in Sbordone et al. (in prep.). To derive 3D-NLTE Li abundances we used the analytical fit as a function of stellar parameters and EW also provided in Sbordone et al. (in preparation). The analysis was also done with 1D model atmospheres, providing essentially the same picture, although $T_{\rm eff}$ in 1D show lower values. We also tried using the Carlsson et al. (1994) NLTE corrections, rather than our own, with no significant difference in the general picture.

In Fig. 2 we display the derived Li abundances versus the effective temperatures of MSs and SGs of the globular cluster NGC 6397. The Li abundance decreases with decreasing temperature, although more rapidly for MSs than for SGs. This Li abundance pattern is different from what is found among field stars (Meléndez & Ramírez 2004; Bonifacio et al. 2007a; González Hernández et al. 2008). The lithium-temperature correlations have a probability of 99.9% and 99.5% for MSs and SGs, respectively, according to the non parametric rank correlation test, Kendall's τ test. We performed a Kolmogorov-Smirnov test and obtained a probability of 8×10^{-6}. Therefore, the possibility that the two sets (MSs and SGs) have been drawn from the same population (same Li abundance) can be rejected. Even ignoring the trend in A(Li) one can deduce that there is a real difference in the A(Li) of MSs and SGs by computing the mean A(Li) and the standard deviation of the mean for the two samples. For SGs we find 2.37 ± 0.01, while for MSs 2.30 ± 0.01. Such a result is also evident in the analysis of Lind et al. (2009) who find only a 0.03 dex difference between the mean A(Li) in MSs and SGs, which is still significant at 1σ. The signal is partly erased by the very narrow range of $T_{\rm eff}$ for MSs deduced by Lind et al. (2009) (~80 K) compared to the wide range (~450 K) for the SGs (see Fig. 7). Such a difference in the $T_{\rm eff}$ range spanned by MSs and SGs is inconsistent with the very similar $B-V$ colours of the two sets of stars. In Fig. 8 online, the lack of correlation between colour and $T_{\rm eff}$ is fully compatible with the photometric and reddening uncertainties. The $T_{\rm eff}$ values adopted by Lind et al. (2009) for the MSs are on the lower $T_{\rm eff}$ side of the range spanned by the sample; this results in an artificial increase of the deduced A(Li) for the MSs, which reduces the difference with SGs, without totally erasing it. We conjecture that this is because the $T_{\rm eff}$ estimates of Lind et al. (2009) are derived by interpolating our V magnitudes onto the cluster fiducial sequence, ignoring any colour information. This necessarily compresses the $T_{\rm eff}$ scale into a range smaller than what is implied by the range in colour, when photometric errors and variations in reddening are taken into account.

4. Discussion and conclusions

Our results imply unambiguously that the Li surface abundance changes with evolutionary status. The fact that A(Li) is higher in SG stars suggests a scenario in which lithium sinks below the photosphere during the MS phase, but to a depth low enough to prevent Li distruction, so that it can be restored in the photosphere, when the stars evolve beyond the TO. The slope of A(Li) with $T_{\rm eff}$ among MS stars suggests that the amount by which Li is depleted in the atmospheres is different for stars of different mass ($T_{\rm eff}$ on the MS). The similar slope found among SG stars suggests that after being restored in the atmosphere at the TO, lithium is then decreased by some other mechanism, possibly mixing linked to the convective motions which are more pronounced for the cooler $T_{\rm eff}$ of the SGs. Although the above described scenario is plausible, we have so far no detailed understanding of the physical processes that bring it about. Diffusive processes may alter the elemental composition of stars. Diffusion has been studied for decades (Aller & Chapman 1960; Michaud et al. 1984), but only a few years ago, detailed element-by-element predictions from models including effects of atomic diffusion and radiative accelerations have become available (Richard et al. 2002). These models produced strong abundance trends that are not compatible with the Spite plateau, and only with the recent inclusion of turbulent mixing, some of the model predictions roughly agree with observations (Richard et al. 2005).

Pure diffusion models (Richard et al. 2005), with no turbulence, predict A(Li) differences as large as 0.4 dex between MSs and SGs of the same age and temperature. The inclusion of turbulence can change this trend, and the SGs may exhibit a A(Li) which is higher, lower, or almost equal to that of the MSs, depending on the precise value of the turbulence parameter.

In Fig. 2 we show the Li isochrones for different turbulent diffusion models (Richard et al. 2005). These models have been shifted up by 0.14 dex in Li abundance to make the initial abundance of the models, $\log(\mathrm{Li/H}) = 2.58$, coincide with the primordial Li abundance predicted from fluctuations of the microwave background measured by the WMAP satellite (Cyburt et al. 2008).

The models assuming pure atomic diffusion, and, among those including turbulent mixing, T6.0 and T6.09, are ruled out by our observations. All such models predict that in MS stars Li should be either more abundant or the same as in subgiant stars. The only model that predicts a A(Li) pattern which is qualitatively similar to that observed, is the T6.25 model. For this model there is a trend of decreasing A(Li) with decreasing $T_{\rm eff}$ and at the cool side MSs show less Li than SGs. However, the model fails quantitatively because A(Li) of the warmest stars is about 0.05 dex lower than what is observed. The slope of A(Li) with $T_{\rm eff}$ is not perfectly reproduced. Models that include atomic

diffusion and tachocline mixing (Piau 2008) do not seem to reproduce our observations, since they provide a constant A(Li) up to 5500 K. The sophisticated models that, besides diffusion and rotation, also take into account the effect of internal gravity waves (Talon & Charbonnel 2004), seem to accurately predict the A(Li) pattern in solar-type stars, at solar metallicity (Charbonnel & Talon 2005). However, Li isochrones have not yet been computed for Population II stars. Our observations call for new investigations into the stellar physics, including gravity waves, atomic diffusion, winds and turbulent mixing. The Li abundance pattern uncovered by our observations has not been observed in field stars and opens up the possibility that it may be peculiar to globular clusters, or, perhaps, to NGC 6397. The cosmological lithium problem still awaits a solution.

Our results indicate a decrease of Li abundance along the subgiant branch, as the stars become cooler and slightly more luminous. This is at variance with what was found by Korn et al. (2007, 2006) and Lind et al. (2009), who find, instead, an *increase* in A(Li) in the same region of the colour-magnitude diagram. We note that the latter authors used our own data, as retrieved from the ESO archive. The difference is mainly in the different $T_{\rm eff}$ scales used by the different investigations. Lind et al. (2009) also estimate slightly different *EW*s for our sample. The difference between their and our weighted mean *EW*s is -0.08 ± 0.02 pm and -0.08 ± 0.03 pm for SG and MS stars, respectively (see also Fig. 5 online) The difference is smaller than the mean error in the *EW* measurements (~0.2 pm in this work and ~0.35–0.4 pm in Lind et al. 2009), suggesting that the two sets of measurements are fully consistent. To verify that the differences in *EW*s are irrelevant to our conclusions we adopted the Lind et al. *EW*s and our $T_{\rm eff}$ to compute A(Li): our main conclusions are unchanged. This reinforces our claim that the difference lies in the $T_{\rm eff}$ scale. The difference in A(Li) that Korn et al. (2006) find between turn-off (TO) and SG stars is driven by the very low $T_{\rm eff}$ they find at the TO. This is inconsistent with our Hα fitting. Our stars are cooler than the TO but we find higher $T_{\rm eff}$ than the TO stars in Korn et al. (2006). We also determined 1D $T_{\rm eff}$ using Hα profiles (see Fig. 6 online). 3D and 1D $T_{\rm eff}$, Li abundances and *EW*s of the stars in our sample are given in Table 2 online. We compare these $T_{\rm eff}$ with the colour temperatures derived from our $B-V$ photometry and the colour calibration, based on the infrared flux method (IRFM) from González Hernández & Bonifacio (2009). Adopting a mean reddening for the cluster of $E(B-V)$=0.186 (Gratton et al. 2003), we find that for our sample of MS stars the mean IRFM effective temperature is 6262 K, to be compared with 6047 K and 6296 K of our 1D and 3D Hα temperatures, respectively. The temperature spread, using both 1D and 3D Hα fitting, is also considerably larger, by a factor of two. That IRFM provides higher $T_{\rm eff}$ than 1D Hα is well established (González Hernández & Bonifacio 2009). We repeated the analysis also with 1D model atmospheres, and the results are qualitatively similar: higher A(Li) for SG stars and decreasing A(Li) for decreasing $T_{\rm eff}$. The first result is very robust, since it can be deduced directly from the distribution of Li *EW*s. The second relies on our ability to model stellar atmospheres. To the extent that our 3D hydrodynamical models are a good description of a stellar atmosphere, the second result is robust as well. The issue of the behaviour of A(Li) with $T_{\rm eff}$ ultimately depends on the $T_{\rm eff}$ scale adopted. This could be solved if we had a direct measure of the angular diameters of metal-poor MSs and SGs. This is probably beyond the reach of present-day interferometers.

NGC 6397 appears to have a higher Li content than field stars of the same metallicity. This needs to be confirmed by a homogeneous analysis of field stars, with the same models and methods. This may or may not be related to the fact that this cluster is nitrogen rich, compared to field stars of the same metallicity (Pasquini et al. 2008).

Acknowledgements. We wish to thank O. Richard for providing us his lithium depletion isochrones for different turbulent diffusion models. Special thanks to K. Lind for sending us her analysis of our data in advance of publication. J. I. G. H., P. B., H.-G. L., N. B. and L. S. acknowledge support from the EU contract MEXT-CT-2004-014265 (CIFIST). We acknowledge use of the supercomputing centre CINECA, which has granted us time to compute part of the hydrodynamical models used in this investigation, through the INAF-CINECA agreement 2006, 2007.

References

Aller, L. H., & Chapman, S. 1960, ApJ, 132, 461
Asplund, M., Lambert, D. L., Nissen, P. E., Primas, F., & Smith, V. V. 2006, ApJ, 644, 229
Barklem, P. S., Piskunov, N., & O'Mara, B. J. 2000, A&A, 363, 1091
Behara, N. T., Ludwig, H.-G., Steffen, M., & Bonifacio, P. 2009, AIP Conf. Ser., 1094, 784
Boesgaard, A. M., Deliyannis, C. P., Stephens, A., & King, J. R. 1998, ApJ, 493, 206
Bonifacio, P., Pasquini, L., Spite, F., et al. 2002, A&A, 390, 91
Bonifacio, P., Molaro, P., Sivarani, T., et al. 2007a, A&A, 462, 851
Bonifacio, P., Pasquini, L., Molaro, P., et al. 2007b, A&A, 470, 153
Carlsson, M., Rutten, R. J., Bruls, J. H. M. J., & Shchukina, N. G. 1994, A&A, 288, 860
Cayrel, R. 1988, The Impact of Very High S/N Spectroscopy on Stellar Physics, IAU Symp., 132, 345
Cayrel, R., Steffen, M., Chand, H., et al. 2007, A&A, 473, L37
Charbonnel, C., & Primas, F. 2005, A&A, 442, 961
Charbonnel, C., & Talon, S. 2005, Science, 309, 2189
Cyburt, R. H., Fields, B. D., & Olive, K. A. 2008, J. Cosmology Astropart. Phys., 11, 12
Freytag, B., Steffen, M., & Dorch, B. 2002, Astron. Nachr., 323, 213
González Hernández, J. I., Bonifacio, P., Ludwig, H.-G., et al. 2008, A&A, 480, 233
González Hernández, J. I., & Bonifacio, P. 2009, A&A, 497, 497
Gratton, R. G., Bonifacio, P., Bragaglia, A., et al. 2001, A&A, 369, 87
Gratton, R. G., Bragaglia, A., Carretta, E., et al. 2003, A&A, 408, 529
Griem, H. R. 1960, ApJ, 132, 883
Hisano, J., Kawasaki, M., Kohri, K., & Nakayama, K. 2009, Phys. Rev. D, 79, 063514
Jedamzik, K. 2004, Phys. Rev. D, 70, 083510
Jedamzik, K. 2006, Phys. Rev. D, 74, 103509
Jittoh, T., Kohri, K., Koike, M., et al. 2008, Phys. Rev. D, 78, 055007
Korn, A. J., Grundahl, F., Richard, O., et al. 2006, Nature, 442, 657
Korn, A. J., Grundahl, F., Richard, O., et al. 2007, ApJ, 671, 402
Lind, K., et al. 2009, A&A, in press
Ludwig, H.-G., Behara, N. T., Steffen, M., & Bonifacio, P. 2009, A&A, 502, L1
Meléndez, J., & Ramírez, I. 2004, ApJ, 615, L33
Michaud, G., Fontaine, G., & Beaudet, G. 1984, ApJ, 282, 206
Molaro, P., & Pasquini, L. 1994, A&A, 281, L77
Pasquini, L., & Molaro, P. 1996, A&A, 307, 761
Pasquini, L., & Molaro, P. 1997, A&A, 322, 109
Pasquini, L., Avila, G., Blecha, A., et al. 2002, The Messenger, 110, 1
Pasquini, L., Bonifacio, P., Molaro, P., et al. 2005, A&A, 441, 549
Pasquini, L., Ecuvillon, A., Bonifacio, P., & Wolff, B. 2008, A&A, 489, 315
Piau, L. 2008, ApJ, 689, 1279
Piau, L., Beers, T. C., Balsara, D. S., et al. 2006, ApJ, 653, 300
Richard, O., Michaud, G., & Richer, J. 2002, ApJ, 580, 1100
Richard, O., Michaud, G., & Richer, J. 2005, ApJ, 619, 538
Sbordone, L., Bonifacio, P., Hernández, J. I., et al. 2008, First Stars III Conference, AIP Conf. Proc., 990, 339
Spergel, D. N., Bean, R., Doré, O., et al. 2007, ApJS, 170, 377
Spite, M., & Spite, F. 1982a, Nature, 297, 483
Spite, F., & Spite, M. 1982b, A&A, 115, 357
Straniero, O., Chieffi, A., & Limongi, M. 1997, ApJ, 490, 425
Talon, S., & Charbonnel, C. 2004, A&A, 418, 1051
Thévenin, F., Charbonnel, C., de Freitas Pacheco, J. A., et al. 2001, A&A, 373, 905
Vidal, C. R., Cooper, J., & Smith, E. W. 1973, ApJS, 25, 37
Wedemeyer, S., Freytag, B., Steffen, M., Ludwig, H.-G., & Holweger, H. 2004, A&A, 414, 1121

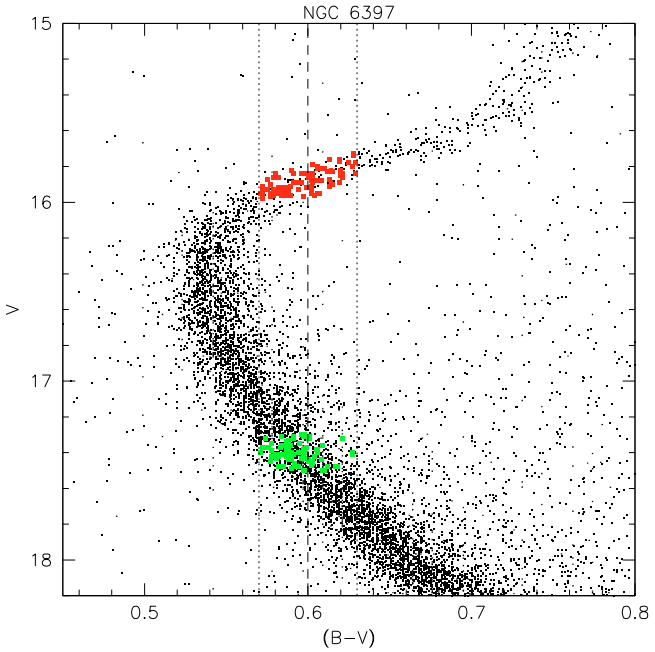

Fig. 3. Colour–magnitude diagram of the cluster NGC 6397. The stars studied in this work are depicted in small filled squares.

Table 1. Details of the 3D hydrodynamical model atmospheres.

$\langle T_{\rm eff}\rangle^a$ [K]	log g [cgs]	[Fe/H] [dex]	Time^b [s]	Snapshots
5500	3.5	–2	46 800	20
5470	4.0	–2	33 800	20
5480	4.5	–2	57 000	20
5860	3.5	–2	112 000	20
5860	4.0	–2	30 000	20
5920	4.5	–2	24 500	18
6290	3.5	–2	82 800	18
6280	4.0	–2	27 600	16
6320	4.5	–2	9100	19
6530	4.0	–2	49 200	20
6530	4.5	–2	9100	19

[a] Temporal average of the emergent $T_{\rm eff}$. [b] Total time covered by the temporal evolution of the photospheric flow sampled at equal intervals in time named as snapshots.

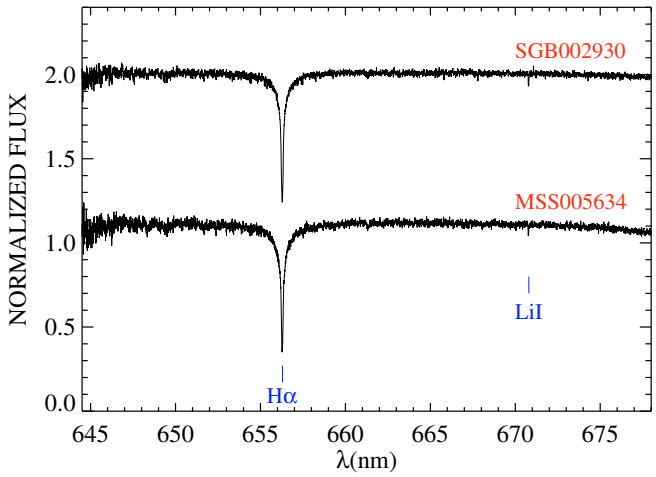

Fig. 4. Observed GIRAFFE/FLAMES spectra of a dwarf star MSS005634 (*bottom*, S/N = 102) and a subgiant star SGB002930 (*top*, S/N = 111)of the globular cluster NGC 6397.

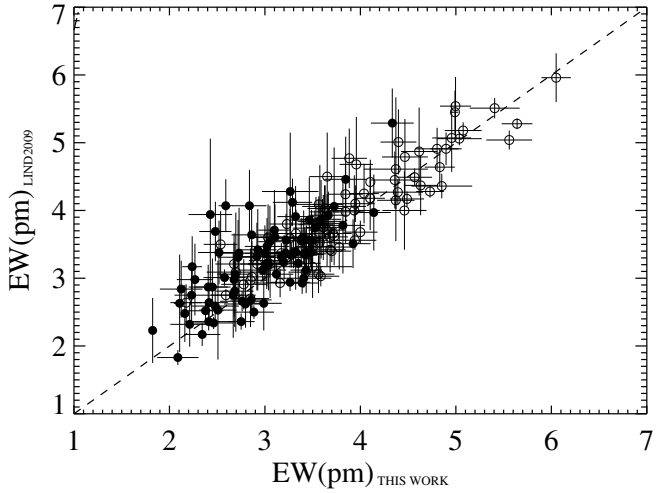

Fig. 5. Comparison between the equivalent widths derived in this work and those provided by Lind et al. (2009). Filled circles and open circles correspond to dwarf and subgiant stars, respectively.

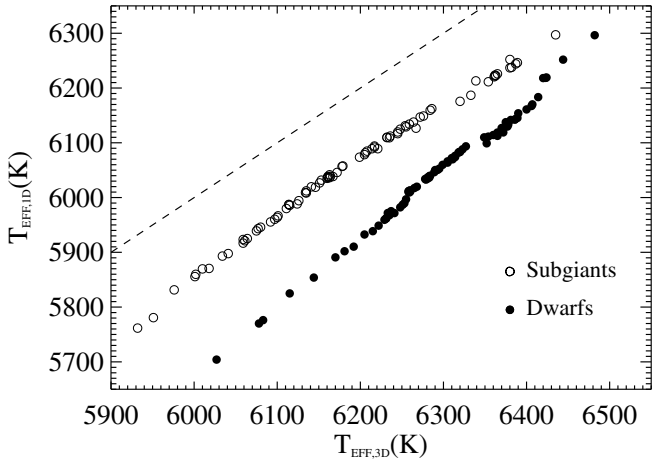

Fig. 6. Comparison between 3D and 1D effective temperatures of the observed stars. Filled circles and open circles correspond to dwarf and subgiant stars, respectively. The dashed line shows the one-to-one relationship.

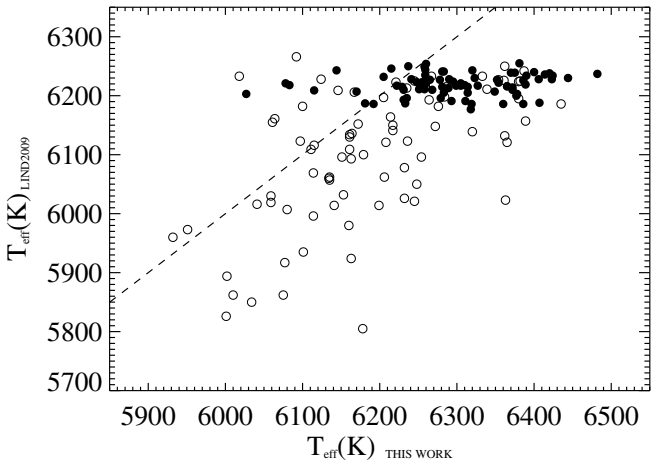

Fig. 7. Comparison between 3D effective temperatures of the observed stars and the 1D effective temperatures derived from colors by Lind et al. (2009). Filled circles and open circles correspond to dwarf and subgiant stars, respectively. The dashed line shows the one-to-one relationship. Since our stars have been selected in a $B-V$ range of 0.06 mag, their temperature range should be of, at least 250 K. It could be larger due to stars being moved into our selection box by photometric and reddening uncertainties. There is no plausible reason why this range should be as small as that implied by the Lind et al. (2009) effective temperatures ~80 K.

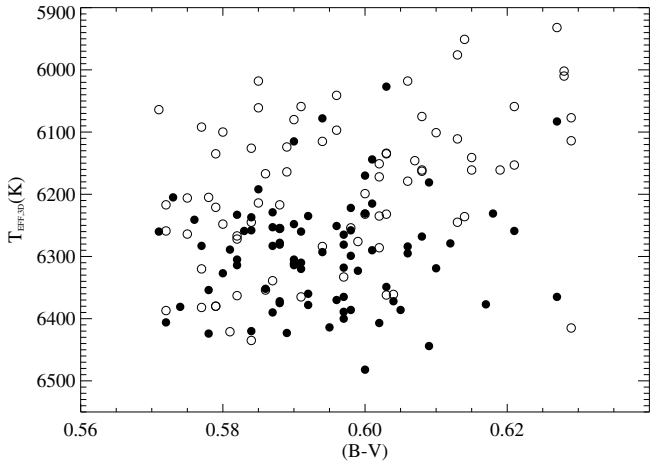

Fig. 8. Comparison between 3D effective temperatures and $B-V$ colours of the observed stars. Filled circles and open circles correspond to dwarf and subgiant stars, respectively. The lack of correlation between $B-V$ and effective temperature is consistent with photometric errors and reddening variations.

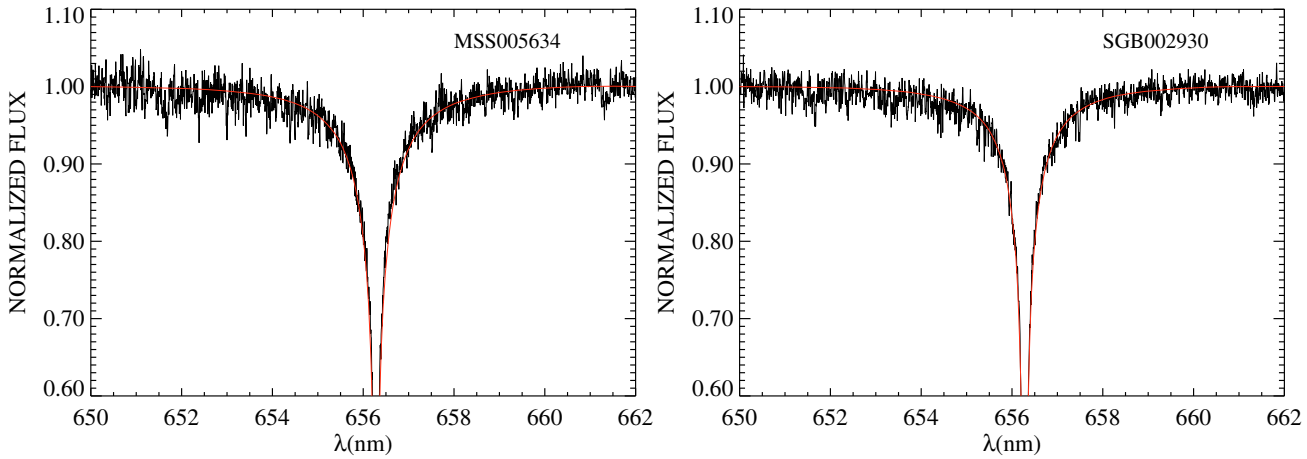

Fig. 9. Observed GIRAFFE/FLAMES Hα profile fitted with a synthetic 3D profile for a dwarf star MSS005634 (*left panel*, S/N = 102, $T_{\rm eff,3D}$ = 6327 K) and for a subgiant star SGB002930 (*right panel*, S/N = 111, $T_{\rm eff,3D}$ = 6126 K).

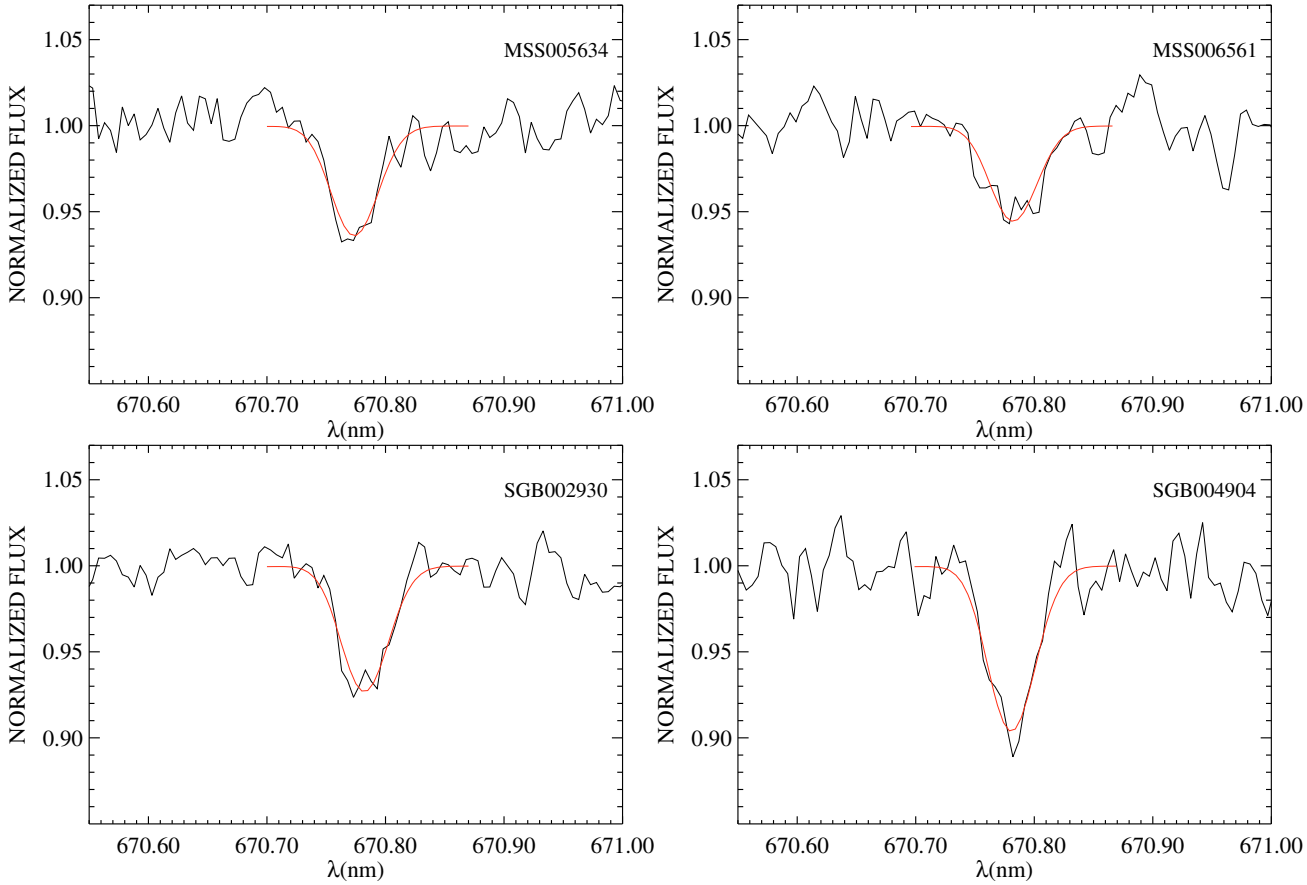

Fig. 10. Observed spectra of two dwarf stars, MSS005634 (*top-left panel*, S/N = 102, EW(Li) = 32.21 mÅ) and MSS006561 (*top-right panel*, S/N = 71, EW(Li) = 27.97 mÅ) and two subgiant stars, SGB002930 (*bottom-left panel*, S/N = 111, EW(Li) = 36.83 mÅ) and SGB004904 (*bottom-left panel*, S/N = 68, EW(Li) = 48.52 mÅ), showing the fit of the Li line with a synthetic profile.

Table 2. Photometric data of the dwarf and subgiant stars of the globular cluster NGC 6397. We also provide the signal-to-noise of the spectra, the 3D and 1D Hα-based effective temperatures, 3D Li abundances, and the equivalent widths and errors.

Star Name	V	$B-V$	SNR	$T_{\rm eff,3D}$ (K)	$T_{\rm eff,1D}$ (K)	EW (mÅ)	δEW^a (mÅ)	δEW^b (mÅ)	$A({\rm Li})_{\rm NLTE,3D}$ (dex)
MSS001253	17.48	0.612	84	6279	6032	32.89	2.06	3.15	2.34
MSS001851	17.38	0.588	86	6278	6033	24.15	1.97	3.10	2.19
MSS002016	17.37	0.576	107	6241	5971	22.32	1.79	2.48	2.13
MSS002882	17.40	0.598	83	6299	6059	22.12	2.03	3.18	2.17
MSS002984	17.40	0.627	84	6365	6118	24.06	2.05	3.14	2.25
MSS003361	17.32	0.600	85	6482	6296	34.06	1.78	3.10	2.51
MSS004052	17.36	0.586	115	6352	6099	30.99	1.69	2.31	2.37
MSS004099	17.38	0.597	82	6265	6017	33.21	1.92	3.22	2.34
MSS004509	17.50	0.597	84	6318	6081	31.94	2.17	3.17	2.36
MSS004829	17.44	0.608	80	6268	6019	27.61	2.31	3.32	2.25
MSS005245	17.30	0.596	115	6370	6127	28.38	1.78	2.31	2.34
MSS005478	17.39	0.587	89	6229	5959	41.40	1.79	2.97	2.42
MSS005528	17.34	0.588	90	6375	6137	25.08	1.94	2.96	2.28
MSS005634	17.41	0.580	102	6327	6093	32.21	1.90	2.60	2.37
MSS005657	17.31	0.584	92	6420	6218	38.46	2.23	2.87	2.52
MSS005755	17.45	0.600	97	6170	5890	33.90	2.07	2.72	2.28
MSS006049	17.43	0.581	83	6289	6046	21.07	0.60	3.19	2.14
MSS006056	17.37	0.572	95	6406	6167	27.51	1.41	2.79	2.35
MSS006236	17.49	0.590	90	6311	6069	24.79	2.49	2.96	2.23
MSS006292	17.39	0.578	85	6354	6111	24.11	2.47	3.11	2.25
MSS006442	17.46	0.592	85	6378	6133	27.19	2.16	3.10	2.32
MSS006561	17.37	0.583	71	6259	6012	27.97	2.25	3.71	2.25
MSS006632	17.40	0.606	78	6284	6039	43.34	2.24	3.41	2.49
MSS006666	17.30	0.598	82	6258	6011	25.77	2.20	3.22	2.21
MSS006761	17.48	0.594	100	6293	6050	36.64	2.01	2.65	2.41
MSS006851	17.32	0.601	92	6144	5853	34.65	1.99	2.89	2.27
MSS006924	17.35	0.578	86	6424	6219	24.63	2.03	3.09	2.31
MSS007267	17.38	0.605	82	6386	6142	26.77	0.29	3.24	2.32
MSS007413	17.37	0.573	95	6205	5932	29.16	1.89	2.80	2.23
MSS007626	17.42	0.582	89	6314	6073	32.63	2.07	2.97	2.37
MSS007823	17.39	0.597	96	6365	6112	25.90	0.75	2.76	2.29
MSS007830	17.34	0.587	98	6390	6153	21.61	0.21	2.71	2.22
MSS007874	17.41	0.591	70	6310	6072	32.99	2.52	3.79	2.37
MSS008138	17.44	0.590	106	6314	6076	24.81	1.69	2.50	2.23
MSS008427	17.41	0.582	80	6305	6063	33.80	1.96	3.31	2.38
MSS013089	17.42	0.597	84	6281	6034	20.88	2.17	3.16	2.13
MSS013492	17.48	0.618	95	6231	5961	29.25	1.97	2.78	2.25
MSS013620	17.31	0.601	97	6215	5938	31.20	1.77	2.73	2.27
MSS013907	17.44	0.600	90	6231	5962	30.52	1.22	2.93	2.27
MSS014243	17.38	0.606	86	6295	6052	32.17	2.40	3.07	2.34
MSS015161	17.50	0.609	79	6181	5901	31.05	2.43	3.37	2.24
MSS015364	17.36	0.609	80	6444	6251	18.24	0.05	3.32	2.18
MSS016174	17.36	0.589	80	6423	6218	31.74	2.09	3.32	2.43
MSS016301	17.32	0.621	94	6259	6009	30.20	1.96	2.81	2.29
MSS016358	17.47	0.602	76	6407	6170	30.22	2.33	3.47	2.39
MSS016481	17.40	0.594	48	6078	5770	37.25	3.35	5.44	2.26
MSS016718	17.41	0.584	86	6258	6010	21.23	2.23	3.09	2.12
MSS016850	17.44	0.588	84	6372	6118	34.32	1.65	3.16	2.43
MSS017006	17.40	0.590	70	6305	6066	29.76	2.47	3.76	2.31
MSS017148	17.37	0.599	102	6323	6088	30.38	2.10	2.61	2.34
MSS017355	17.33	0.588	125	6281	6036	33.90	1.67	2.12	2.36
MSS018410	17.32	0.591	99	6320	6083	33.49	2.34	2.68	2.38
MSS019380	17.42	0.587	77	6253	5989	33.22	2.03	3.45	2.33
MSS019711	17.40	0.588	82	6255	5996	30.00	2.14	3.22	2.28
MSS019748	17.50	0.598	89	6386	6142	35.23	2.32	2.98	2.46
MSS019966	17.48	0.592	77	6360	6114	28.85	2.10	3.44	2.34

Table 2. continued.

Star Name	V	$B-V$	SNR	$T_{\rm eff,3D}$ (K)	$T_{\rm eff,1D}$ (K)	EW (mÅ)	δEW^a (mÅ)	δEW^b (mÅ)	$A({\rm Li})_{\rm NLTE,3D}$ (dex)
MSS020053	17.48	0.617	63	6377	6129	27.29	2.43	4.21	2.32
MSS020239	17.44	0.590	62	6115	5824	32.65	2.96	4.25	2.22
MSS020289	17.45	0.603	100	6349	6109	35.75	2.32	2.66	2.44
MSS020400	17.42	0.604	116	6372	6126	26.84	1.98	2.29	2.31
MSS020449	17.42	0.590	69	6248	5982	28.55	2.15	3.84	2.25
MSS020824	17.32	0.574	89	6381	6141	26.87	1.87	2.98	2.32
MSS020882	17.48	0.582	65	6233	5971	26.68	2.35	4.08	2.21
MSS024313	17.38	0.597	78	6389	6145	35.88	2.10	3.39	2.47
MSS024953	17.46	0.603	93	6027	5704	24.28	2.28	2.86	2.01
MSS025117	17.31	0.591	91	6260	6013	23.43	1.90	2.90	2.17
MSS025164	17.43	0.596	86	6251	5986	22.38	1.04	3.10	2.14
MSS025647	17.31	0.597	121	6400	6160	34.88	1.68	2.20	2.46
MSS026667	17.45	0.577	90	6283	6036	38.17	2.31	2.94	2.42
MSS029201	17.41	0.627	80	6083	5776	22.67	1.90	3.30	2.02
MSS029608	17.48	0.585	80	6192	5910	32.80	2.68	3.31	2.28
MSS036470	17.50	0.610	77	6319	6083	34.19	2.20	3.44	2.39
MSS036731	17.35	0.595	101	6414	6183	24.50	1.91	2.63	2.30
MSS037695	17.40	0.571	66	6260	6010	25.19	2.19	4.01	2.20
MSS037993	17.45	0.601	95	6290	6050	39.23	1.84	2.79	2.44
MSS038318	17.36	0.584	100	6237	5975	29.88	1.88	2.64	2.27
MSS044623	17.40	0.587	89	6283	6039	23.78	1.88	2.97	2.19
MSS047718	17.48	0.592	69	6235	5967	34.07	2.90	3.83	2.33
MSS049487	17.43	0.598	71	6222	5948	28.61	2.11	3.73	2.23
SGB001167	15.94	0.587	108	6339	6213	25.91	1.73	2.46	2.29
SGB001953	15.96	0.604	86	6361	6220	30.33	2.06	3.09	2.39
SGB002243	15.94	0.602	91	6286	6162	37.28	0.19	2.90	2.43
SGB002302	15.89	0.614	120	6236	6112	41.04	0.08	2.22	2.44
SGB002675	15.88	0.603	109	6232	6109	36.24	1.53	2.44	2.38
SGB002902	15.95	0.578	102	6205	6078	29.19	1.79	2.61	2.25
SGB002930	15.95	0.584	111	6126	5994	36.83	1.64	2.39	2.31
SGB003140	15.95	0.580	77	6100	5963	31.59	2.73	3.42	2.21
SGB003332	15.88	0.608	69	6161	6038	43.92	2.64	3.82	2.42
SGB003371	15.96	0.579	94	6380	6236	36.79	1.91	2.82	2.50
SGB003553	15.86	0.621	82	6059	5916	48.03	2.25	3.22	2.39
SGB003556	15.90	0.615	68	6161	6036	39.42	2.25	3.88	2.37
SGB003678	15.91	0.589	117	6164	6038	35.58	1.71	2.27	2.32
SGB003852	15.95	0.585	47	6018	5870	34.99	4.16	5.61	2.20
SGB003854	15.89	0.603	104	6362	6223	34.34	1.62	2.54	2.45
SGB003930	15.95	0.582	106	6267	6126	30.19	1.88	2.51	2.31
SGB004063	15.84	0.629	68	6114	5986	50.36	2.35	3.90	2.46
SGB004228	15.87	0.613	98	6111	5980	45.68	1.82	2.72	2.41
SGB004239	15.84	0.596	118	6041	5897	35.74	1.84	2.24	2.23
SGB004288	15.93	0.584	65	6435	6297	34.79	2.55	4.05	2.51
SGB004474	15.86	0.603	110	6134	6009	38.83	1.85	2.40	2.34
SGB004549	15.94	0.588	90	6255	6129	26.77	1.97	2.96	2.25
SGB004699	15.83	0.613	95	6245	6119	36.03	2.03	2.80	2.39
SGB004904	15.84	0.598	68	6254	6131	48.52	3.19	3.86	2.55
SGB005126	15.88	0.602	85	6151	6026	49.90	0.35	3.12	2.48
SGB005198	15.89	0.596	75	6097	5960	44.66	2.40	3.52	2.38
SGB005333	15.88	0.608	106	6163	6036	34.28	1.58	2.50	2.30
SGB005417	15.94	0.572	90	6259	6134	32.01	1.78	2.96	2.34
SGB005556	15.82	0.620	110	6114	5987	56.41	1.61	2.41	2.52

Table 2. continued.

Star Name	V	$B-V$	SNR	$T_{\rm eff,3D}$ (K)	$T_{\rm eff,1D}$ (K)	EW (mÅ)	δEW^a (mÅ)	δEW^b (mÅ)	$A({\rm Li})_{\rm NLTE,3D}$ (dex)
SGB005765	15.84	0.600	99	6199	6073	21.75	1.65	2.66	2.11
SGB005947	15.92	0.588	95	6217	6092	36.11	1.86	2.78	2.37
SGB006102	15.86	0.582	70	6363	6222	26.95	3.05	3.78	2.33
SGB006281	15.89	0.619	122	6161	6037	25.36	1.77	2.17	2.15
SGB006305	15.86	0.600	96	6232	6110	39.47	2.03	2.78	2.42
SGB006463	15.93	0.594	141	6284	6159	40.38	1.55	1.88	2.47
SGB006585	15.97	0.577	109	6382	6237	28.64	1.65	2.44	2.37
SGB006625	15.84	0.603	88	6135	6012	49.56	2.04	3.02	2.47
SGB006673	15.96	0.586	98	6167	6038	31.72	1.81	2.72	2.26
SGB007322	15.95	0.579	108	6221	6089	34.99	1.91	2.45	2.35
SGB007495	15.84	0.591	88	6059	5923	43.71	1.96	3.01	2.34
SGB007501	15.86	0.579	86	6135	6008	33.25	2.17	3.10	2.26
SGB007624	15.80	0.627	64	5932	5761	55.59	2.40	4.13	2.37
SGB007674	15.89	0.594	75	6115	5985	43.60	2.50	3.54	2.38
SGB008019	15.87	0.575	113	6206	6081	41.02	1.54	2.34	2.42
SGB008043	15.92	0.599	117	6276	6148	34.27	1.81	2.26	2.38
SGB008308	15.97	0.597	101	6333	6186	35.85	1.94	2.62	2.45
SGB008491	15.90	0.577	92	6320	6175	36.52	1.88	2.87	2.45
SGB008808	15.91	0.572	100	6217	6094	34.55	1.61	2.65	2.34
SGB013359	15.78	0.629	129	6077	5943	49.96	1.63	2.06	2.43
SGB014992	15.95	0.571	100	6064	5925	35.61	1.66	2.65	2.24
SGB015032	15.93	0.585	66	6061	5921	35.64	2.56	3.99	2.24
SGB015177	15.93	0.579	102	6380	6252	30.54	1.56	2.60	2.40
SGB015392	15.96	0.586	85	6354	6211	37.14	1.95	3.13	2.48
SGB015418	15.82	0.614	98	5951	5780	34.30	1.68	2.70	2.14
SGB015847	15.81	0.610	131	6101	5966	39.99	1.80	2.03	2.33
SGB016013	15.82	0.590	75	6080	5945	44.61	2.31	3.55	2.37
SGB016363	15.95	0.577	71	6092	5955	32.63	2.35	3.74	2.22
SGB016701	15.83	0.615	109	6141	6019	47.29	1.45	2.44	2.45
SGB016858	15.98	0.572	82	6387	6244	28.49	1.94	3.22	2.37
SGB016871	15.73	0.628	139	6010	5869	60.50	1.54	1.91	2.48
SGB016936	15.91	0.602	117	6172	6045	37.78	1.69	2.26	2.35
SGB017040	15.74	0.628	114	6002	5859	48.31	1.58	2.33	2.35
SGB017100	15.83	0.612	51	5703	5506	43.71	3.35	5.16	2.06
SGB017116	15.96	0.589	82	6124	5988	35.34	1.84	3.24	2.29
SGB018051	15.93	0.575	88	6264	6137	35.09	1.96	3.02	2.39
SGB018096	15.92	0.585	96	6214	6089	37.00	2.04	2.75	2.38
SGB018128	15.84	0.621	90	6153	6031	46.31	1.76	2.95	2.45
SGB018930	15.88	0.606	92	6179	6057	36.31	1.86	2.87	2.34
SGB019686	15.89	0.591	131	6365	6225	34.16	1.54	2.03	2.45
SGB019890	15.95	0.607	106	6146	6018	44.88	1.78	2.49	2.42
SGB020001	15.76	0.613	124	5976	5831	57.08	1.46	2.15	2.42
SGB020304	15.84	0.580	100	6248	6124	39.57	1.75	2.66	2.44
SGB024422	15.81	0.608	101	6075	5939	48.97	1.63	2.62	2.41
SGB024914	15.95	0.602	72	6235	6109	27.78	2.35	3.68	2.25
SGB025290	15.92	0.582	103	6272	6146	38.43	1.81	2.57	2.44
SGB025764	15.96	0.584	89	6245	6116	28.50	1.60	2.99	2.27
SGB026642	15.81	0.606	62	6160	6035	39.36	2.67	4.24	2.37
SGB029317	15.79	0.603	96	6001	5855	50.76	1.93	2.76	2.38
SGB029417	15.77	0.619	82	6034	5893	38.45	1.87	3.23	2.26
SGB030350	15.76	0.619	62	6178	6056	54.06	2.62	4.29	2.55
SGB030403	15.91	0.613	100	6389	6246	36.51	1.91	2.64	2.50
SGB031394	15.96	0.572	92	6362	6222	32.30	1.81	2.88	2.42
SGB032079	15.78	0.625	89	6163	6041	43.98	1.88	2.97	2.43
SGB036901	15.95	0.606	82	6208	6084	46.15	1.91	3.21	2.48

[a] Error of the equivalent width measurements estimated from a fitting routine that uses as free parameters the velocity shift, the continuum location, and the equivalent width of the Li line. [b] Error of the equivalent width associated to the signal-to-noise ratio and the wavelength dispersion of the spectra, derived using Cayrel's formula (Cayrel 1988).